CSAP Acts as a Regulator of TTLL-Mediated Microtubule Glutamylation

Guillaume Bompard, Juliette van Dijk, Julien Cau, Yoann Lannay, Guillaume Marcellin, Aleksandra Lawera, Siem van Der Laan, Krzysztof Rogowski

Article

Cell Reports

CSAP Acts as a Regulator of TTLL-Mediated Microtubule Glutamylation

Graphical Abstract

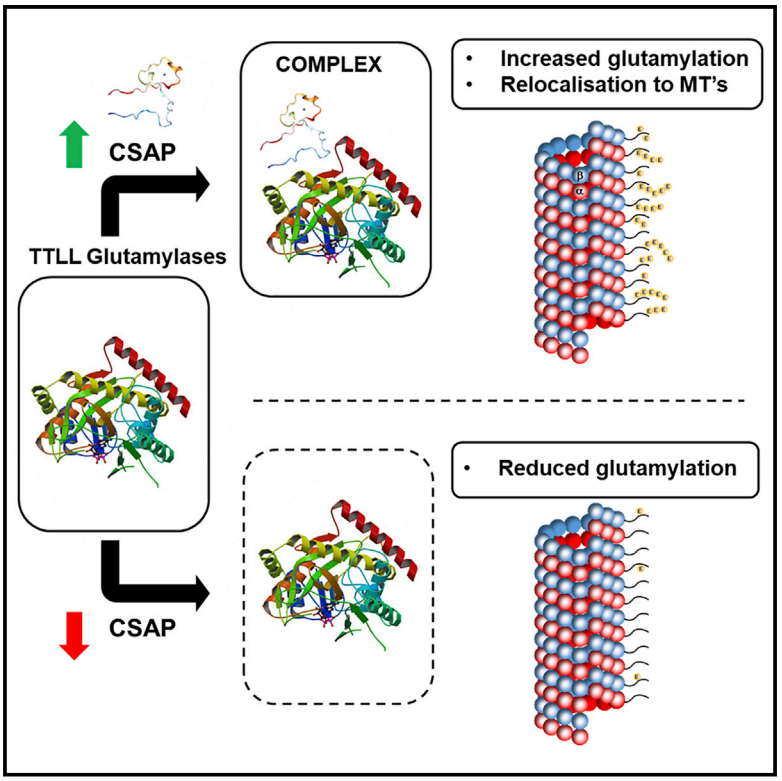

Authors

Guillaume Bompard, Juliette van Dijk, Julien Cau, ..., Aleksandra Lawera, Siem van der Laan, Krzysztof Rogowski

Correspondence

krzysztof.rogowski@igh.cnrs.fr

In Brief

Bompard et al. describe an activator of tubulin glutamylases that modify the microtubule-based cytoskeleton. They find that CSAP forms a complex with TTLL5, which controls its localization and activity on microtubules.

Highlights

- CSAP interaction with microtubules is independent of their glutamylation status
- TTLL5 and CSAP form a complex
- CSAP promotes relocalization of TTLL5 to microtubules
- CSAP is an activator of all autonomously active TTLL glutamylases

Bompard et al., 2018, Cell Reports *25*, 2866–2877
December 4, 2018
https://doi.org/10.1016/j.celrep.2018.10.095

CellPress

OPEN ACCESS
CellPress

Cell Reports
Article

CSAP Acts as a Regulator of TTLL-Mediated Microtubule Glutamylation

Guillaume Bompard,[1] Juliette van Dijk,[1,2] Julien Cau,[1] Yoann Lannay,[1] Guillaume Marcellin,[1] Aleksandra Lawera,[1,3] Siem van der Laan,[1] and Krzysztof Rogowski[1,4,*]

[1]Institute of Human Genetics (IGH), UMR9002 CNRS-University of Montpellier, 34094 Cedex 5, 141 Rue de la Cardonille, 34090 Montpellier, France

[2]Present address: Montpellier Cell Biology Research Center (CRBM), UMR5237 CNRS-University of Montpellier, 1919 Route de Mende, 34293 Montpellier, France

[3]Present address: Department of Medicine, University of Cambridge, Addenbrooke's Hospital, Hills Road, Cambridge CB2 0SP, UK

[4]Lead Contact

*Correspondence: krzysztof.rogowski@igh.cnrs.fr

https://doi.org/10.1016/j.celrep.2018.10.095

SUMMARY

Tubulin glutamylation is a reversible posttranslational modification that accumulates on stable microtubules (MTs). While abnormally high levels of this modification lead to a number of disorders such as male sterility, retinal degeneration, and neurodegeneration, very little is known about the molecular mechanisms underlying the regulation of glutamylase activity. Here, we found that CSAP forms a complex with TTLL5, and we demonstrate that the two proteins regulate their reciprocal abundance. Moreover, we show that CSAP increases TTLL5-mediated glutamylation and identify the TTLL5-interacting domain. Deletion of this domain leads to complete loss of CSAP activating function without impacting its MT binding. Binding of CSAP to TTLL5 promotes relocalization of TTLL5 toward MTs. Finally, we show that CSAP binds and activates all of the remaining autonomously active TTLL glutamylases. As such, we present CSAP as a major regulator of tubulin glutamylation and associated functions.

INTRODUCTION

Microtubules (MTs) are protein tubes formed by non-covalent association of αβ-tubulin heterodimers. An important feature of MTs that allows them to adapt to a number of essential functions, such as cell division, maintaining cell shape, intracellular transport, and cell motility, is dynamic instability. Dynamic instability is characterized by the ability to undergo alternating phases of end growth and shrinkage (Bowne-Anderson et al., 2015), a phenomenon that is controlled by a myriad of factors including MT-associated proteins (MAPs) and molecular motors (Bowne-Anderson et al., 2015). Posttranslational modifications (PTMs) of MTs are thought to play a central role in regulating the binding of interacting proteins. Among them, glutamylation consists of the generation of glutamate side chains of variable length that are added to the γ-carboxyl groups of the primary sequence glutamate residues, located within the C-terminal tails of both α- and β-tubulin (Janke, 2014). The C-terminal tails of tubulin protrude from the surface of MTs where they act as binding sites for a number of MT-interacting proteins. As such, glutamylation provides a rapid and reversible way of regulating the interaction between MAPs and MTs. For example, increased glutamylation enhances the processivity of kinesin-1 and 2 (O'Hagan et al., 2011; Sirajuddin et al., 2014) and increases the activity of ciliary dynein (Kubo et al., 2010; Suryavanshi et al., 2010) and MT-severing enzymes, namely spastin and katanin (Lacroix et al., 2010; Sharma et al., 2007). In addition, glutamylation appears to modulate the binding of MAP1 and MAP2 (Bonnet et al., 2001). Finally, glutamylation has been proposed to promote association to MTs of the newly identified MAP called cilia and spindle-associated protein (CSAP) (Backer et al., 2012; Ohta et al., 2015), which plays an important role in zebrafish development (Backer et al., 2012).

Historically, glutamylation has been detected using a monoclonal antibody (GT335) that recognizes the branching-point glutamate and thus all side chains regardless of their length (Wolff et al., 1994). These studies have established that increased GT335 staining is associated with long-lived MTs, including those present in centrioles, axonemes, and neuronal projections, but also mitotic spindles (Janke, 2014). Although the majority of MTs are highly dynamic, a small population undergoes stabilization and is likely to play a key role in several important processes, such as cell morphology, motility, differentiation, and viral infection (Ayala et al., 2007; Gundersen et al., 1989; Sabo et al., 2013).

The level of glutamylation in the cells is established by competition between the forward enzymes belonging to the tubulin tyrosine ligase-like (TTLL) family defined by the presence of conserved TTL domain (Janke et al., 2005; van Dijk et al., 2007), and the reverse enzymes belonging to the cytosolic carboxypeptidase (CCP) family (Rogowski et al., 2010; Tort et al., 2014). Up to date, all sequenced mammalian genomes have been found to encode nine TTLL glutamylases and six homologs of the CCP family (Janke, 2014; Yu et al., 2015). Among the glutamylases, TTLL5 is the most ubiquitously

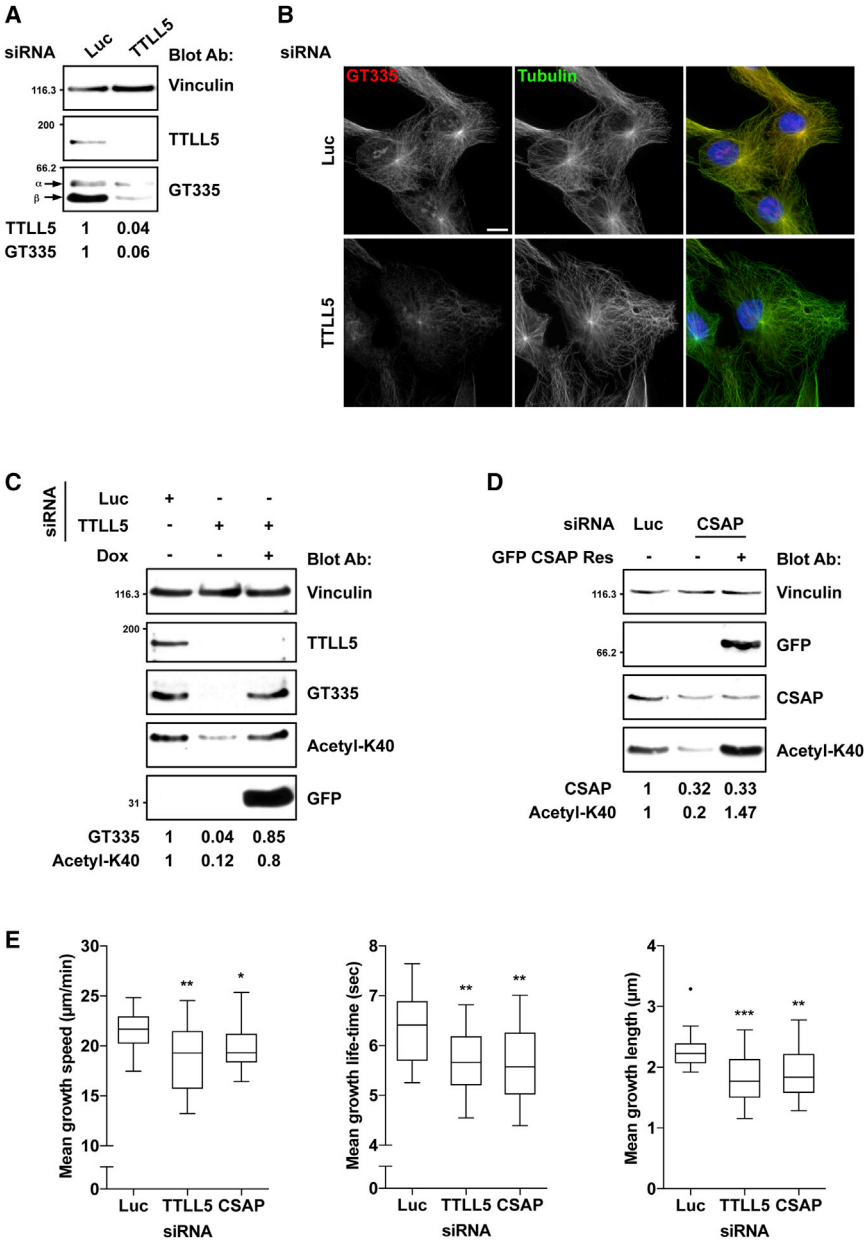

Figure 1. Depletions of TTLL5 or CSAP Affect MT Dynamics

(A) TTLL5 depletion significantly affects microtubule (MT) glutamylation. Representative immunoblot analyses of protein extracts from Luc- (control) and TTLL5-depleted RPE-1 cells. Vinculin staining is used to demonstrate equal loading. α and β indicate the position of α/β tubulins. Normalized quantification of TTLL5 and GT335 signals are indicated below.

(B) Representative images of RPE-1 cells depleted for Luc or TTLL5 stained for tubulin and glutamylation (GT335). Scale bar: 10 μm.

(C) mTTLL5 expression rescues MT glutamylation and acetylation. Representative immunoblot analyses of protein extracts from control Luc- and TTLL5-depleted RPE-1 FRT/T-Rex mTTLL5 IRES GFP cells expressing (Dox, doxycycline) or not mTTLL5. Note that TTLL5 antibody does not recognize mTTLL5, in which expression is evaluated by GFP expression. Normalized quantification of GT335 and acetyl-K40 signals are indicated below.

(D) CSAP expression rescues MT acetylation. Representative immunoblot analyses of protein extracts from control Luc- and CSAP-depleted RPE-1 cells expressing or not GFP CSAP Res (siRNA resistant). Normalized quantification of CSAP and acetyl-K40 signals are indicated below.

(E) Depletions of TTLL5 or CSAP affect MT dynamics. Boxplots representing the distribution of mean growth speed (left), growth lifetime (middle), and growth length (right) of EB3-GFP tracked comets per single cell treated with indicated siRNA (Luc representing the control conditions throughout the article). For details, see Table S1. In boxplots, whiskers are set at 1.5 times the interquartile range, horizontal lines mark the median, and boxes indicate interquartile range (25%–75%). The dot indicates an outlier, which was beyond whisker range (n = 3; Student's t test p values are indicated in Table S1; *p < 0.05, **p < 0.01, ***p < 0.001 throughout the article).

expressed (van Dijk et al., 2007), and mutations of this gene, which reduce the level of glutamylation, have been associated with male sterility and retinal degeneration (Bedoni et al., 2016; Lee et al., 2013; Sergouniotis et al., 2014). Interestingly, also abnormally high MT glutamylation, caused by the mutations in CCP1, leads to numerous pathological conditions, such as neurodegeneration, retinal degeneration, or male sterility (Rogowski et al., 2010).

However, very little is known about the molecular mechanisms involved in the regulation of glutamylase activity. Here, we show that TTLL5 and CSAP exist in a complex and reciprocally regulate one another's abundance. We demonstrate that the binding of CSAP to TTLL5 increases glutamylation and promotes relocalization of TTLL5 toward MTs. Finally, we present evidence that CSAP interacts and activates all of the remaining autonomously active glutamylases, further underlying the general importance of CSAP as the regulator of tubulin glutamylation.

RESULTS

TTLL5 and CSAP Regulate MT Dynamics and Stability

Depletion of TTLL5 in RPE-1 cells, using small interfering RNA (siRNA), resulted in an almost complete loss of tubulin glutamylation (Figures 1A and 1B), confirming that TTLL5 is a major glutamylating enzyme. Besides decreasing tubulin glutamylation, knockdown of TTLL5 also led to a strong reduction in the levels of K40 α-tubulin acetylation (acetyl-K40; Figures 1C and S1A), suggesting that TTLL5 plays an important role in regulation

of MT stability. Importantly, reduction in both tubulin modifications was rescued by expression of mouse TTLL5, which is insensitive to the siRNA used (Figure 1C). The most straightforward explanation of reduced MT stability following TTLL5 knockdown, is that diminished glutamylation negatively affects the binding of a MT stabilizing MAP(s). One potential candidate is CSAP, whose MT association in HeLa cells was previously shown to be regulated by TTLL5 (Backer et al., 2012). In agreement, using immunofluorescence, we found that in cells depleted for TTLL5, the level of MT-associated CSAP was strongly diminished (Figures S1B and S1C). This raised the possibility that CSAP might be responsible for decreased MT stability in TTLL5-depleted cells. To verify this hypothesis, we identified an siRNA that efficiently reduced the levels of CSAP expression (Figure 1D). Similar to depletion of TTLL5, knockdown of CSAP strongly reduced the level of acetyl-K40 (Figure 1D). Moreover, expression of an siRNA-resistant mutant of CSAP in RPE-1 cells depleted for the endogenous protein fully restored the level of acetyl-K40 (Figure 1D).

To better understand the role of glutamylation in MT dynamics, we used a previously generated RPE-1 cell line stably expressing end binding 3 (EB3) protein fused to GFP (EB3-GFP) to track growing MT ends (Thoma et al., 2010). The key MT characteristics, such as growth speed, lifetime, and length, were measured using plusTipTracker software in both TTLL5- and CSAP-depleted cells (Applegate et al., 2011). Representative images of EB3-GFP comets detection and tracking are shown in Figure S1D. In TTLL5-depleted cells, we observed a significant reduction of average MT growth speed (13%), lifetime (12%), and length (20%) (Figure 1E; Table S1), suggesting that TTLL5 promotes MT polymerization and/or MT stabilization. Highly similar changes in the dynamic parameters of MTs were observed upon the knockdown of CSAP (Figure 1E; Table S1). To better understand how changes in specific parameters translate into the collective behavior of the entire MT population, we categorized individual MTs based on their growth speed and lifetime. We classified MTs into four subpopulations: (1) slow and short-lived, (2) slow and long-lived, (3) fast and short-lived, and (4) fast and long-lived. As compared to controls, cells depleted for TTLL5 or CSAP had a reduced number of long-lived MT sub-tracks (both slow and fast; dark and light red) with a concomitant increase in the number of short-lived MTs (both slow and fast; dark and light blue, Figure S1E). This result is consistent with a general reduction of MT stability in cells depleted for either TTLL5 or CSAP.

CSAP Binds MTs Independently of Glutamylation Status

By alignment of the human, mouse, and zebrafish CSAP protein sequences, we identified five distinct evolutionarily conserved regions, among which one was located in the N-terminal part, while the remaining four are in the C terminus of the protein (Figures 2A and S2A). Moreover, computation of the theoretical isoelectric point (pI) of the full-length and the N-terminal and C-terminal parts of human CSAP showed substantial disparities in acidity. While the N-terminal part of CSAP is enriched in highly acidic residues (pI = 4.34), the C-terminal region is mainly composed of basic amino acids residues (pI = 10.92). Since MTs exhibit negative charges on their surface, this suggests that CSAP is likely to interact with MTs through its positively charged C-terminal domain. To test this hypothesis, we expressed either a full-length protein, the N-terminal domain, or the C-terminal domain of CSAP fused to GFP. As expected, the full-length CSAP and its C-terminal domain co-localized with MTs, while the N-terminal fragment showed a diffused cytoplasmic localization (Figure 2B). In order to biochemically substantiate these observations, we carried out co-sedimentation assays using purified brain MTs and a recombinant full-length CSAP or its two domains fused to glutathione S-transferase (GST) (Figure S2B). In agreement with immunofluorescence results (Figure 2B), we found that full-length CSAP and its C-terminal domain co-sedimented with MTs, while the N-terminal fragment remained in the supernatant (Figure 2C).

Since CSAP appeared to act as a classical MAP, we tested whether it promotes MT assembly by lowering the critical concentration of tubulin required for polymerization. To this end, we performed an *in vitro* MT assembly assay, in the presence or absence of CSAP using an amount of tubulin below the critical concentration. The N-terminal fragment of CLIP170 (Nt-CLIP170) containing the MT-binding domain (Figure S2C), which has previously been shown to promote MT assembly (Gupta et al., 2009), was used as a positive control. CSAP promoted MT assembly with a similar efficiency as CLIP170 (Figure S2D), confirming that it indeed has the properties of a classical MT-stabilizing MAP. Next, we examined whether the binding of CSAP to MTs is regulated by glutamylation. Using co-sedimentation assays, we first determined the affinity of CSAP for MTs that have been polymerized using Sf9-derived tubulin (Widlund et al., 2012). An apparent affinity of 2.63 μM was calculated (Figures 2D and 2E), corroborating previously published values determined using brain MTs (Backer et al., 2012). Next, we examined whether the binding of CSAP to MTs is affected by glutamylation. To test this hypothesis in an unbiased manner, we isolated tubulin either from Sf9 cells, which have no detectable glutamylation, or from their counterparts overexpressing TTLL5 (Figure 2F). Using fixed amounts of CSAP at a concentration below its apparent K_d (1 μM), we performed co-sedimentation assays with increasing amounts of MTs prepared from differentially modified tubulin. Surprisingly, we did not observe any effect of the glutamylation status on the binding of CSAP to MTs (Figure 2F).

TTLL5 and CSAP Are a Part of the Same Complex

Since CSAP did not preferentially bind glutamylated MTs (Figure 2F), an alternative hypothesis that may explain the localization of CSAP to modified MTs (Backer et al., 2012) is that it forms a complex with glutamylating enzymes such as TTLL5. Thus, we co-expressed TTLL5 GFP and hemagglutinin (HA) CSAP in HEK293T cells and performed immunoprecipitations using either anti-HA or anti-GFP antibodies. We detected an interaction between CSAP and TTLL5 regardless of the antibodies used (Figures 3A and 3B). Next, we attempted to identify the region of CSAP that is responsible for the binding to TTLL5. We co-expressed TTLL5 GFP with either a full-length HA CSAP or its N- or C-terminal domains in HEK293 cells. Using GFP-based immunoprecipitation, we found that only full-length CSAP and its C-terminal part were efficiently co-precipitated with TTLL5

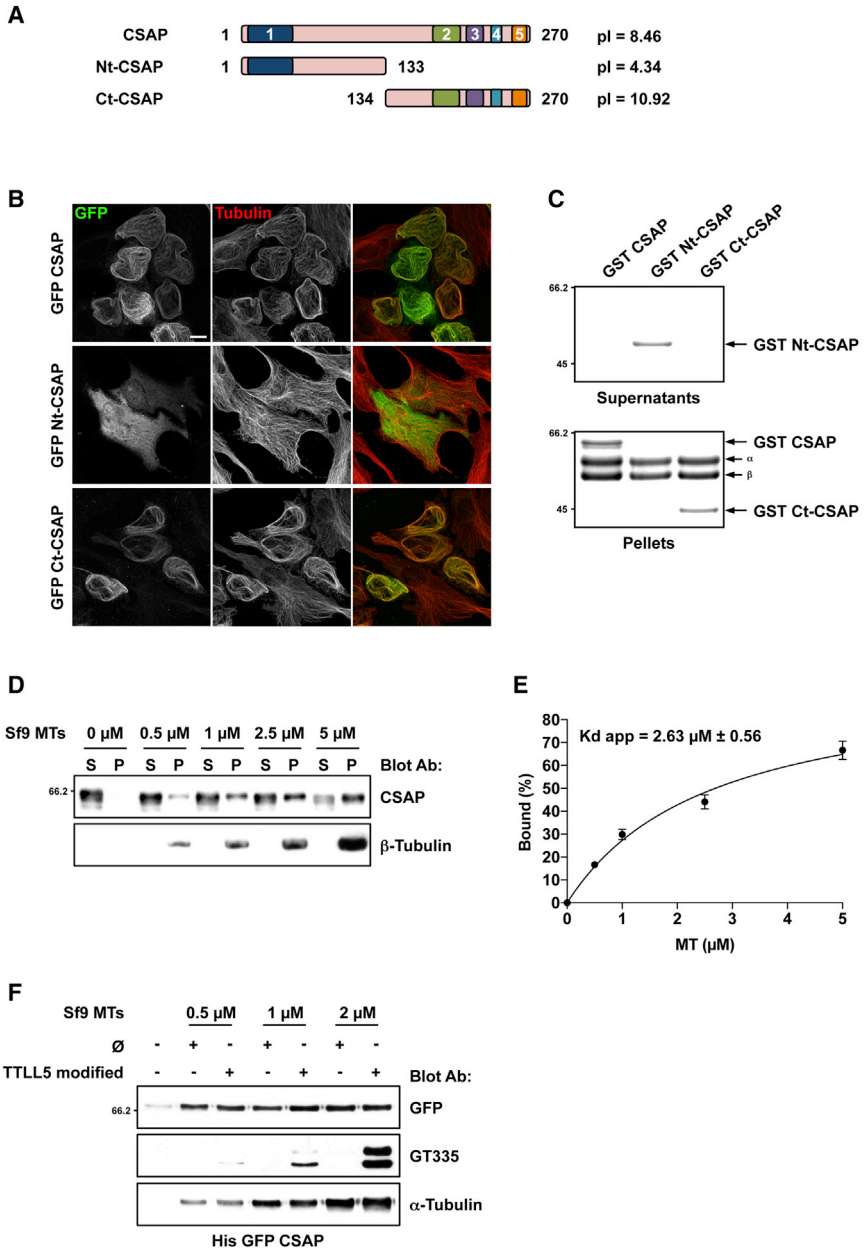

Figure 2. CSAP Is a MAP Binding MTs Independently of Their Glutamylation Status

(A) Schematic representation of human CSAP and its two fragments. The position of respective amino acids and isoelectric point are indicated. Boxes numbered 1 to 5 depict evolutionarily conserved sequences (see Figure S2A).

(B) CSAP localizes to MTs through its C-terminal (Ct) sequence. Maximum intensity projection of RPE-1 cells overexpressing either full-length, Nt-, or Ct-CSAP protein fused to GFP stained for tubulin. Scale bar: 10 µm.

(C) CSAP binds to MTs through its C-terminal sequence. Coomassie blue-stained protein gels showing a representative result of MT co-sedimentation assay with GST-tagged full-length CSAP or its two fragments as depicted in (A). α and β indicate tubulins. Note that only full-length CSAP and its C- but not the N-terminal domain are co-sedimented.

(D) Determination of CSAP affinity to MTs. Representative immunoblot analyses of MT co-sedimentation assay using GST CSAP (1 µM) and indicated concentration of Sf9 MTs.

(E) Graph quantifying the MT co-sedimentation of GST CSAP. The line represents the theoretical curve for a bimolecular interaction (n = 3; means ± SEM). The apparent dissociation constant (K_d app) was calculated using Prism 7 software (one site – specific binding).

(F) CSAP binding to MTs is not regulated by glutamylation. Representative immunoblot analyses of MT co-sedimentation assay using His GFP CSAP (1 µM) and MT prepared from tubulins purified from Sf9 or Sf9 cells expressing His TTLL5. Note that no detectable glutamylation was observed on MTs obtained from untreated Sf9 cells.

(Figure 3B), indicating that the N-terminal part does not bind this enzyme. Reciprocally, we tested which parts of TTLL5 interacts with CSAP. We divided TTLL5 into two fragments, the N-terminal part encompassing the TTL domain with the surrounding sequences that are required for its enzymatic activity, and the remaining C-terminal tail (Figure 3C). Pull-down analysis of GFP-tagged TTLL5 fragments revealed that both the N- and the C-terminal domains of TTLL5 interacted with GST CSAP (Figure 3D). However, a preferential interaction of CSAP was observed for the N-terminal fragment of TTLL5 containing the TTL domain (Figure 3D). Binding of the N-terminal part of TTLL5 to CSAP was further confirmed with GST pull-down assays using recombinant proteins (Figures S3A and S3B).

To test whether the interaction between these two proteins was dependent on TTLL5 activity, we expressed either active or enzymatically "dead" (E366G) TTLL5 GFP in HEK293T cells and performed GST pull-downs. Immunoblot analysis showed that GST CSAP efficiently precipitated TTLL5 GFP regardless of its enzymatic activity (Figure S3C). Often, when two proteins are a part of the same complex, a depletion of one component affects the abundance of its partner subunit (Steffen et al., 2006). Strikingly, knockdown of TTLL5 not only diminished the levels of tubulin glutamylation but also the amount of CSAP (Figure 3E). Conversely, depletion of CSAP diminished the levels of TTLL5 as well as tubulin glutamylation (Figure 3E). Similar results were obtained in two additional human cell lines (Figure S3D), further reinforcing the existence of the complex. Collectively, the data suggest that the reduction in MT-associated CSAP (Figures S1B and S1C) is independent of glutamylation and most likely reflects a change in the overall protein levels of CSAP.

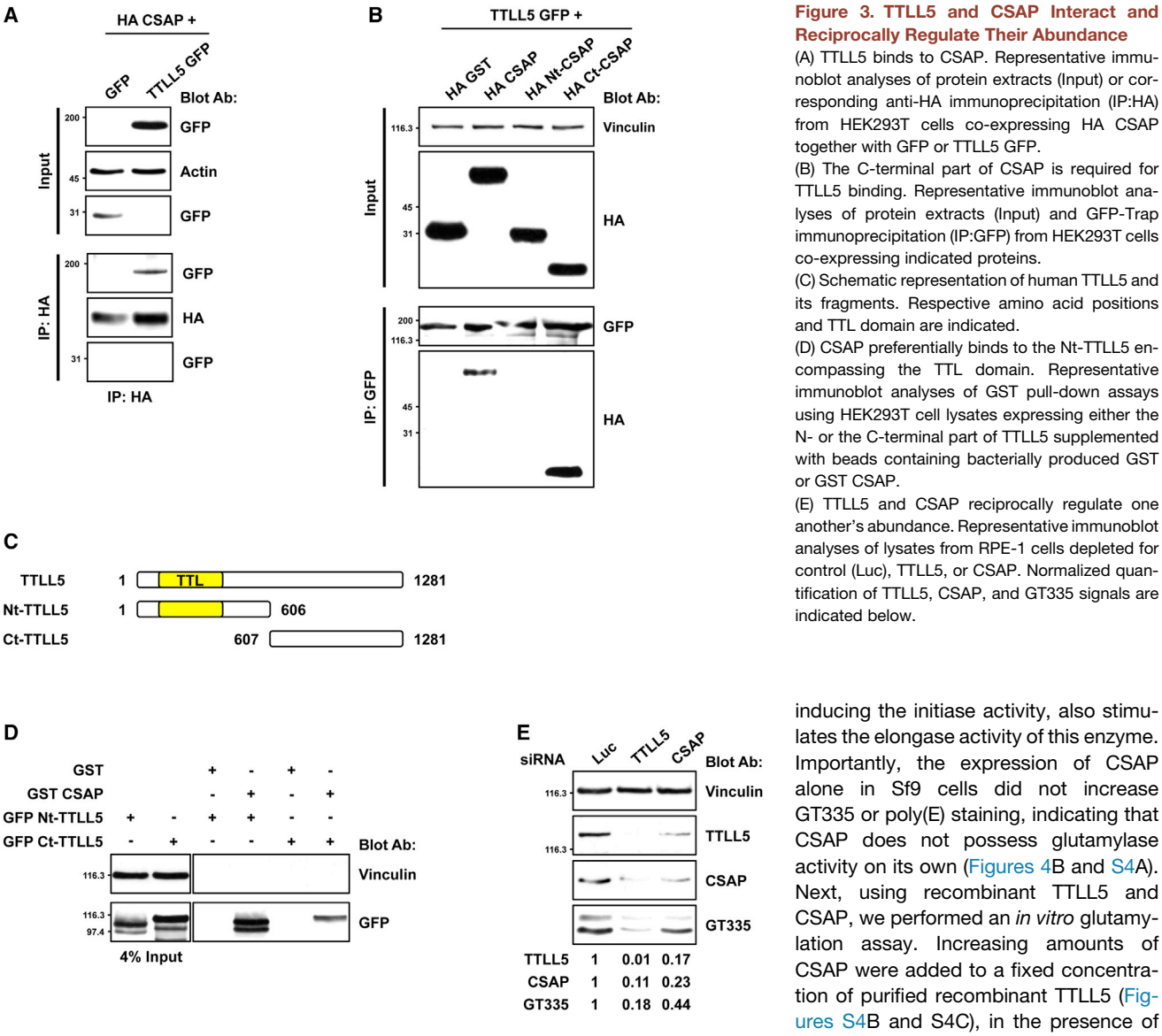

Figure 3. TTLL5 and CSAP Interact and Reciprocally Regulate Their Abundance

(A) TTLL5 binds to CSAP. Representative immunoblot analyses of protein extracts (Input) or corresponding anti-HA immunoprecipitation (IP:HA) from HEK293T cells co-expressing HA CSAP together with GFP or TTLL5 GFP.

(B) The C-terminal part of CSAP is required for TTLL5 binding. Representative immunoblot analyses of protein extracts (Input) and GFP-Trap immunoprecipitation (IP:GFP) from HEK293T cells co-expressing indicated proteins.

(C) Schematic representation of human TTLL5 and its fragments. Respective amino acid positions and TTL domain are indicated.

(D) CSAP preferentially binds to the Nt-TTLL5 encompassing the TTL domain. Representative immunoblot analyses of GST pull-down assays using HEK293T cell lysates expressing either the N- or the C-terminal part of TTLL5 supplemented with beads containing bacterially produced GST or GST CSAP.

(E) TTLL5 and CSAP reciprocally regulate one another's abundance. Representative immunoblot analyses of lysates from RPE-1 cells depleted for control (Luc), TTLL5, or CSAP. Normalized quantification of TTLL5, CSAP, and GT335 signals are indicated below.

CSAP Is an Activator of TTLL5 Enzymatic Activity

Having established that CSAP binds to TTLL5, we next asked whether this affects the enzymatic activity of TTLL5. Therefore, we expressed TTLL5 alone or in combination with full-length CSAP, the N-terminal fragment, or the C-terminal fragment. Immunoblots revealed that co-expression of TTLL5 with full-length CSAP, or its C-terminal domain, led to a strong increase in its chain-initiating glutamylase activity as demonstrated with GT335 labeling (Figure 4A). In contrast, co-expression of TTLL5 with the N-terminal part did not affect glutamylase activity. Surprisingly, as shown by the poly(E) labeling (an antibody that recognizes long glutamate chains), we also observed that, in the presence of CSAP or its C-terminal fragment, TTLL5 had higher chain-elongating activity (Figure 4A). Similar results were obtained in Sf9 cells co-infected with baculoviruses expressing TTLL5 in combination with CSAP fused to two different tags (Figures 4B and S4A). This suggests that CSAP, apart from inducing the initiase activity, also stimulates the elongase activity of this enzyme. Importantly, the expression of CSAP alone in Sf9 cells did not increase GT335 or poly(E) staining, indicating that CSAP does not possess glutamylase activity on its own (Figures 4B and S4A). Next, using recombinant TTLL5 and CSAP, we performed an *in vitro* glutamylation assay. Increasing amounts of CSAP were added to a fixed concentration of purified recombinant TTLL5 (Figures S4B and S4C), in the presence of Taxol-stabilized MTs and radioactively labeled glutamate. Strikingly, we observed a dose-dependent increase of TTLL5 activity by CSAP demonstrating its direct role in regulating TTLL5 glutamylase activity (Figure 4C).

CSAP Directs TTLL5 Enzymatic Activity toward MTs

We then studied whether the effect of CSAP on TTLL5 activity was specific to MTs or also detectable with other substrates. To address this point, we tested TTLL5 activity in the presence or absence of CSAP on either ectopically expressed or endogenous glutamylation substrates, including NAP2, SET, RanGAP1, and PELP1 (van Dijk et al., 2008). We did not observe any increase in the TTLL5 activity toward any of the substrates tested (Figures S5A–S5D), suggesting that induction of TTLL5 activity by CSAP is specific to MTs.

One way in which CSAP could direct TTLL5 activity toward MTs is simply by promoting their stabilization. This would allow a prolonged access of the modifying enzyme to the substrate

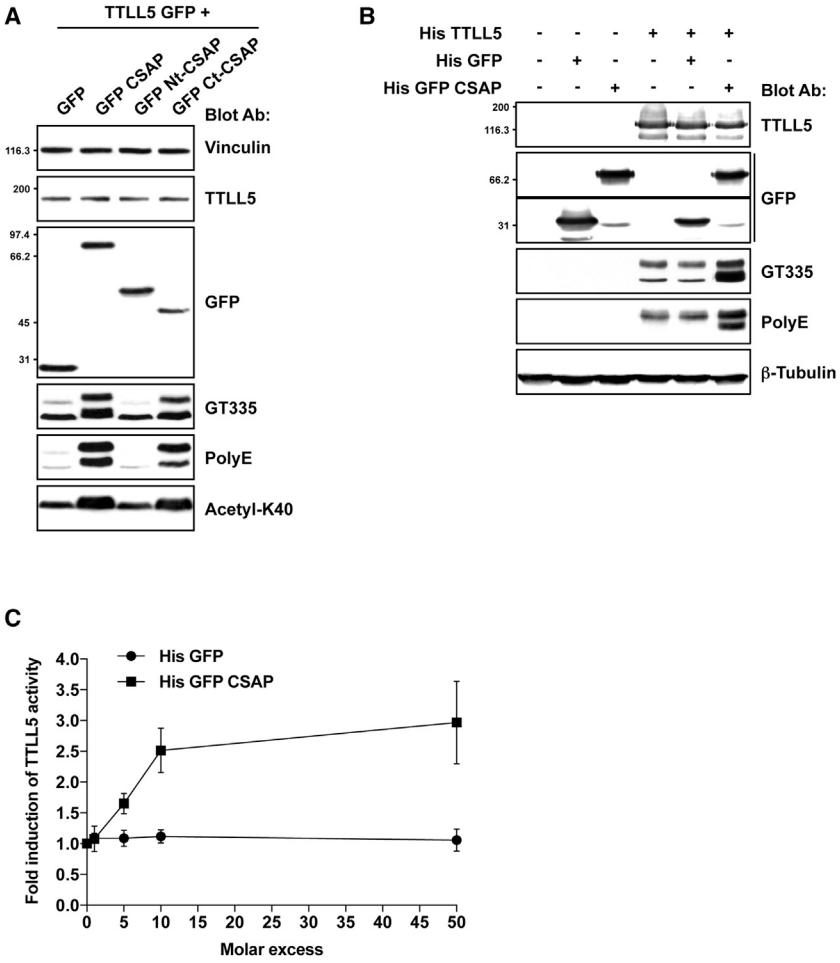

Figure 4. CSAP Regulates Glutamylase Activity of TTLL5

(A) Binding of CSAP to TTLL5 stimulates its glutamylase activity. Representative immunoblot analyses of lysates from HEK293T cells co-expressing TTLL5 GFP either with GFP alone or with various GFP-tagged CSAP-derived proteins as depicted in Figure 2A.

(B) CSAP is triggering TTLL5 activation in insect cells. Representative immunoblot analyses of protein extracts from Sf9 cells overexpressing His TTLL5 in combination with His GFP (control) or His GFP CSAP.

(C) *In vitro* glutamylation assay showing direct stimulation of TTLL5 activity by CSAP. Graph showing fold induction of HA GST TTLL5 activity measured *in vitro* in the presence of indicated molar excess of His GFP or His GFP CSAP (n = 4; means ± SEM).

and as consequence lead to an increase in overall glutamylation level. A similar mechanism has been recently described for MEC-17, the enzyme that catalyzes acetyl-K40 (Szyk et al., 2014). To test this hypothesis, we co-expressed TTLL5 with either CSAP, Tau, or MAP2D. As anticipated, co-expression of either CSAP, MAP2D, or Tau resulted in a strong accumulation of acetyl-K40 (Figure S5E), suggesting that all three MAPs increase MT stability. However, in contrast to CSAP, presence of Tau or MAP2D did not alter TTLL5 glutamylase activity (Figures S5E and S5F), indicating that TTLL5 activation by CSAP is independent of MT stabilization.

Previous studies have demonstrated that TTLL5, when expressed alone, shows no apparent association with MTs except for centrosomes (van Dijk et al., 2007). This is in a stark contrast to overproduced CSAP that displays clear co-localization with MTs (Figure 2B). Therefore, we compared cellular localization of TTLL5 alone, or in the presence of CSAP or MAP2D. Since overexpression of an active TTLL5 induced MT severing, we used a catalytically "dead" version of TTLL5 (E366G). Co-expression of TTLL5 (E366G) with CSAP led to a striking re-localization of TTLL5 to MTs in all cells expressing the two proteins (Figure 5A), whereas MAP2D did not alter cellular distribution of TTLL5. Next, we tested whether re-localization of TTLL5 induced by CSAP could affect the partitioning of glutamylation between free tubulin and MTs. We expressed TTLL5 either alone, or in combination with CSAP or MAP2D, and performed cell fractionation assays. When TTLL5 was expressed alone, or in the presence of MAP2D, the glutamylation signal was detected in both the soluble (tubulin) and insoluble (MTs) fractions (Figure 5B). Remarkably, when TTLL5 was expressed in the presence of CSAP, glutamylation was found exclusively in the MT fraction despite a considerable increase in its levels (Figure 5B).

Based on previously identified evolutionarily conserved domains in the C-terminal part of CSAP protein (Figure S2A), we deleted one of the domains and analyzed the TTLL5-mediated glutamylation in the presence of the internally deleted CSAP (Figure 5C). Strikingly, while CSAP Δ178–204 still increased acetyl-K40, it did not display any effect on TTLL5 activity (Figure 5D). Immunofluorescence analysis comparing the cellular distribution of both full-length CSAP and CSAP Δ178–204 showed that both proteins associated with MTs in a similar manner (Figure 5E), suggesting that this domain is critically involved in interaction with TTLL5. Finally, pull-down analysis of TTLL5 with recombinant CSAP proteins confirmed lack of interaction between CSAP Δ178–204 and TTLL5 (Figures 5F and S5G). Altogether, our data demonstrate that CSAP regulates TTLL5 by recruiting the enzyme to its substrate and by specifically stimulating glutamylase activity on MTs.

CSAP Is a Regulator of All Autonomously Active TTLL Glutamylases

Given that CSAP associated preferentially with the part of TTLL5 that encompassed the TTL domain, we wondered whether it could also bind to other TTLL glutamylases. Therefore, we expressed GFP-tagged versions of all of the remaining autonomously active glutamylases, including TTLL4, TTLL6, TTLL7, TTLL11, and TTLL13, as well as TTL. Cell lysates were incubated with glutathione beads containing GST CSAP to assess

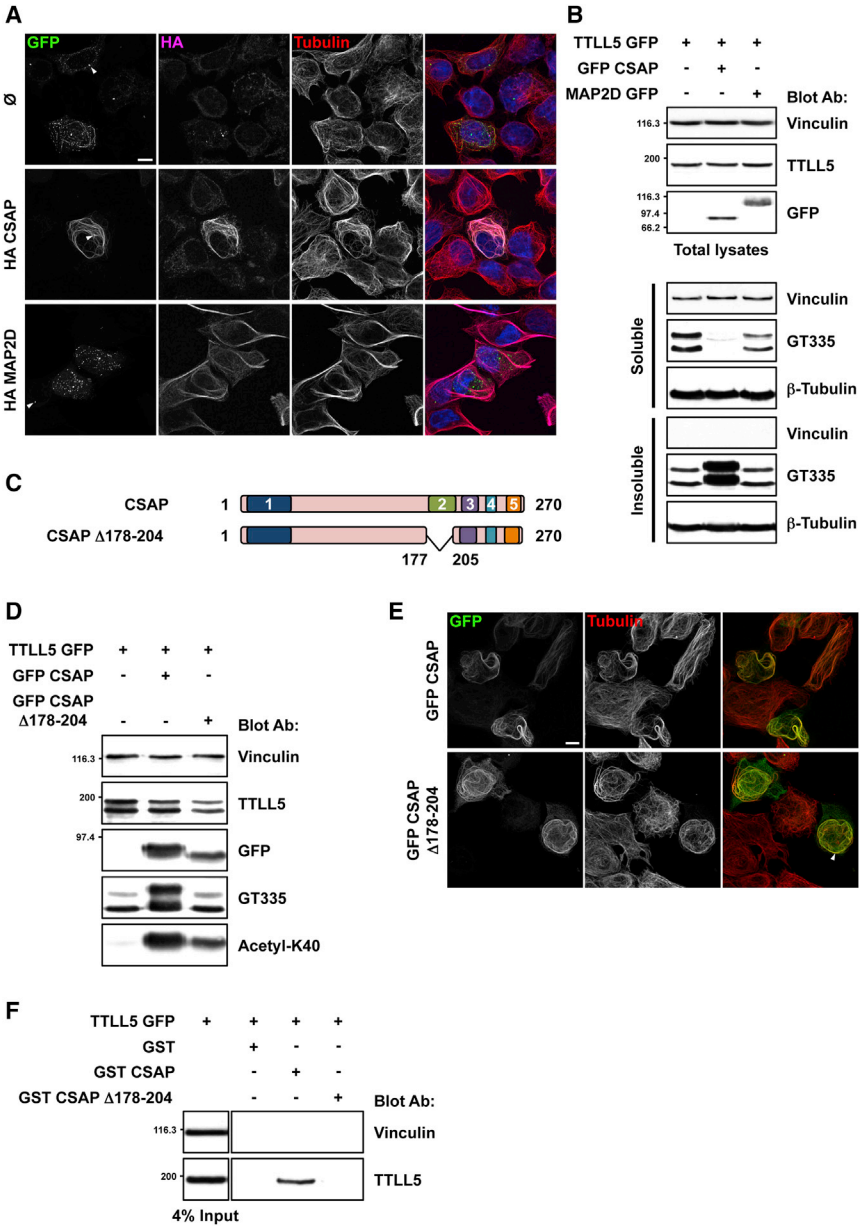

Figure 5. CSAP Promotes TTLL5 Association with MTs

(A) CSAP promotes MT localization of TTLL5. Maximum intensity projection of RPE-1 cells co-expressing TTLL5 (E366G) GFP in combination with HA, HA CSAP, or HA MAP2D stained for tubulin and HA. Scale bar: 10 μm. Arrowheads indicate the position of centrosomes, which in the absence of CSAP are the major sites of TTLL5 accumulation.

(B) CSAP alters substrate specificity of TTLL5. Representative immunoblot analyses of fractionation experiment using protein extracts from HEK293T cells overexpressing TTLL5 GFP alone, with GFP CSAP or MAP2D GFP. The cells were separated into soluble and insoluble fractions containing tubulin and MT, respectively. Vinculin labeling was used to monitor the fidelity of fractionation.

(C) Schematic representation of CSAP and the internal deletion CSAP Δ178–204 lacking the second evolutionarily conserved domain described in Figures 2A and S2A.

(D) CSAP residues 178–204 are required for TTLL5 activation but not for the increase of tubulin acetylation. Representative immunoblot analyses of lysates from HEK293T cells overexpressing TTLL5 GFP in combination with GFP CSAP WT or Δ178–204 mutant.

(E) CSAP Δ178–204 mutant co-localizes with MTs. Maximum intensity projection of RPE-1 cells overexpressing GFP CSAP WT or Δ178–204 stained for tubulin. Arrowhead indicates CSAP and MTs co-localization. Scale bar: 10 μm.

(F) CSAP residues 178–204 are required for TTLL5 binding. Representative immunoblot analyses of GST pull-down assays using HEK293T cell lysates expressing TTLL5 GFP supplemented with beads containing bacterially produced GST or GST CSAP WT or Δ178–204.

interaction with the individual glutamylases. Following pull-downs, immunoblot analyses showed that all glutamylases tested specifically bound to GST CSAP, whereas TTL did not (Figure 6A). The interaction was further confirmed for TTLL7 and TTLL11 using recombinant proteins (Figures S6A–S6C). Next, we tested whether binding resulted in increased glutamylase activity. Therefore, we expressed all of the above-mentioned autonomously active glutamylases, either alone or in combination with CSAP. Strikingly, we observed that CSAP strongly increased glutamylation activity of all enzymes tested as shown by immunoblotting analysis using GT335 or poly(E) antibodies (Figures 6B and S6D). Interestingly, both increase in initiation (GT335) and elongation activity (poly[E]) were observed for TTLL6, TTLL7, TTL11, and TTLL13, while for TTLL4 only increase in initiation was detected. Next, since CSAP appeared to act as a general regulator of glutamylase activity, we wanted to test whether it also regulates the stability of other glutamylases. Thus, we sought for a cell line in which, apart from TTLL5, there was a high expression of another glutamylating enzyme. Based on the transcript-level analysis of TTLL5 and TTLL7 in five different human cell lines (Figure 6C), we studied the effect of CSAP knockdown in SH-SY5Y cells, a human neuroblastoma cell line. In agreement with our interaction data, CSAP depletion resulted in a reduction of not only TTLL5 but also TTLL7 protein levels (Figure 6D). Similar results were obtained in RPE-1 cells where TTLL7 is not a dominant glutamylase (Figure S6E). Taken together, our data support a model in which CSAP acts as a critical regulator of TTLL-mediated tubulin glutamylation.

CSAP Induces Severing Activity

One of the best-documented functions of tubulin glutamylation in cells is the regulation of MT-severing enzymes such as spastin

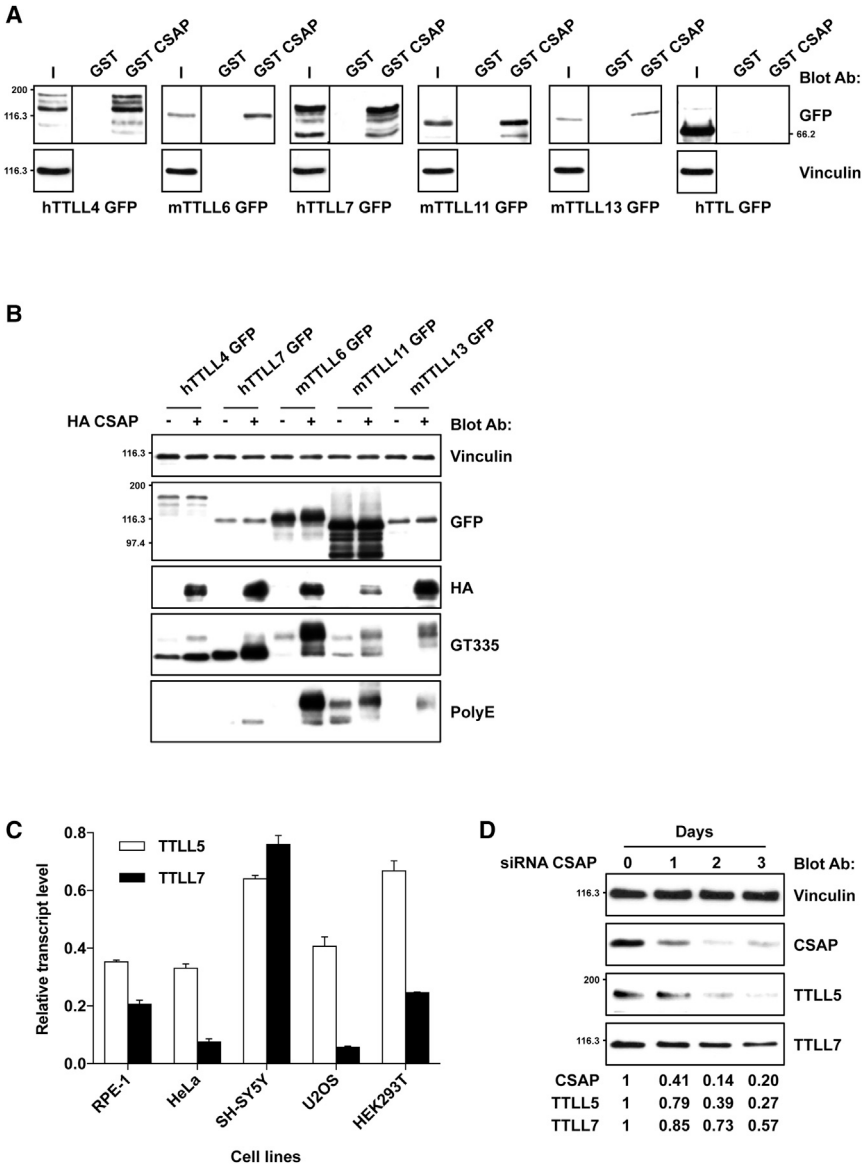

Figure 6. CSAP Binds and Stimulates the Activity of All Autonomously Active Tubulin Glutamylases

(A) CSAP interacts with all autonomously active glutamylases but not with TTL. Representative immunoblot analyses of GST or GST CSAP pull-down experiment using protein extracts from HEK293T overexpressing indicated TTLL (mouse, m; human, h) fused to GFP.

(B) CSAP stimulates glutamylase activity of all autonomously active glutamylases. Representative immunoblot analyses of extracts from HEK293T overexpressing indicated TTLL fused to GFP in combination with (+) or without (–) HA CSAP.

(C) SH-SY5Y cells express high levels of TTLL7. TTLL5 and TTLL7 transcript expression levels were determined by RT-qPCR to characterize a cell line with high TTLL7 expression as compared to TTLL5 (n = 3; mean ± SD).

(D) CSAP depletion alters TTLL5 and TTLL7 expressions in SH-SY5Y. Representative immunoblot analyses of protein extracts from Luc- (control) and CSAP-depleted SH-SY5Y neuroblastoma cells after indicated days of siRNA treatment. Normalized quantification of CSAP, TTLL5, and TTLL7 signals are indicated below.

DISCUSSION

In this study, we show that tubulin glutamylation is linked to MT dynamics. Our key finding is that TTLL5, an autonomously active glutamylase, exists in a complex with CSAP. The two partners regulate their mutual abundance and the presence of CSAP greatly increases the enzymatic activity of TTLL5. Current view limits regulation of tubulin glutamylation to the balance between the activity of glutamylating and deglutamylating enzymes and does not integrate additional regulators (Janke, 2014; Yu et al., 2015). Our work identifies a new mechanism involving a TTLL-interacting protein, which has the ability to profoundly alter the level of this modification by activating both initiating and elongating activities.

and katanin (Lacroix et al., 2010; Sharma et al., 2007; Valenstein and Roll-Mecak, 2016). Since CSAP increased the activity of several tubulin glutamylases, we wondered whether this stimulation could facilitate glutamylation-dependent MT severing. Initially, we set out to test this hypothesis using TTLL5 in U2OS cells as previously described (Lacroix et al., 2010). However, expression of TTLL5 alone was sufficient to induce extensive MT severing. Therefore, we the used TTLL13, the enzyme previously reported to have the weakest activity among the autonomously active glutamylases (van Dijk et al., 2007). We expressed TTLL13 GFP either alone or together with HA CSAP (Figure 7A) and scored the number of cells with extensively severed MTs in both conditions. We found that the presence of CSAP increased the number of cells with severed MTs by about 4-fold (Figure 7B). Overall, activation of tubulin glutamylases by co-expression of CSAP promoted MT severing.

Backer and colleagues showed that CSAP preferentially associates with glutamylated MTs and proposed that it acts as an effector of glutamylation. This interpretation was based on the observed disappearance of CSAP from the MTs in the absence of TTLL5 (Backer et al., 2012). We found that tubulin glutamylation has no effect on the binding of CSAP to MTs (Figure 2F) and that reduction in MT-associated CSAP most likely is to be explained by the observation that TTLL5 and CSAP form a complex in which both proteins mutually regulate their abundance (Figure 3E). Furthermore, we have shown that reciprocal stabilization also occurs with TTLL7 (Figure 6D). Considering that CSAP binds and activates

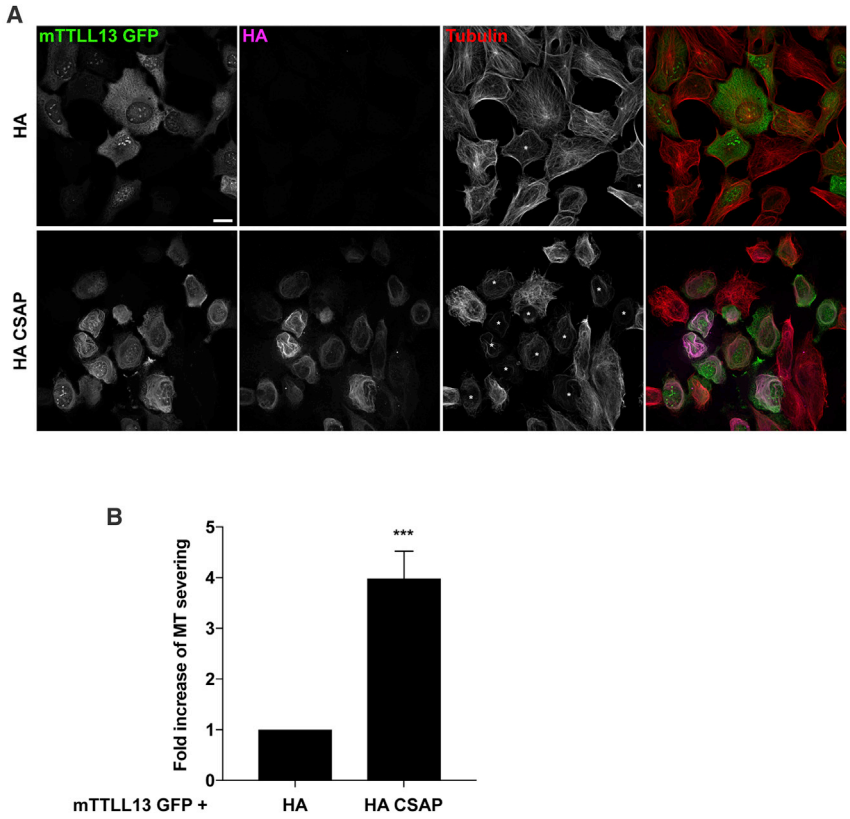

Figure 7. CSAP Regulates MT Severing Induced by MT Glutamylation

(A) CSAP activates TTLL13 activity and promotes MT severing. Maximum intensity projection of U2OS cells expressing mTTLL13 GFP alone or in combination with HA CSAP stained for tubulin and HA. The white asterisk (*) indicates cells displaying MT severing. Scale bar: 20 μm.

(B) Graph representing fold increase of MT severing in cells expressing mTTLL13 GFP alone or with CSAP as shown in (B) (n = 5; means ± SEM. ***p = 0.0005. A total of around 500 cells per condition were analyzed).

all of the remaining autonomously active glutamylases (Figure 6A), it suggests that the same mechanism is likely to apply to other TTLLs.

Some of the enzymes involved in glutamylation are inactive upon overexpression, likely because they require additional subunits (Janke et al., 2005; van Dijk et al., 2007). For example, TTLL1, the only glutamylase that was identified by classical biochemistry, forms a complex with four additional proteins (Janke et al., 2005). One of them, PGs1, appears to be important for TTLL1 activity as the mice lacking this protein display reduced levels of glutamylation in the brain (Ikegami et al., 2007). Thus, PGs1 may be involved in the regulation of stability and/or the activity of TTLL1. However, since it does not localize to MTs upon overexpression (Regnard et al., 2003), it is unlikely to have a similar function as CSAP. As for the other components of the TTLL1 complex, it remains an open question whether any of them can directly bind to MTs.

Studies in *Chlamydomonas* have shown that another non-autonomous glutamylase, TTLL9, forms a complex with a flagella-associated protein (FAP234), which is required for its stability and flagellar localization (Kubo et al., 2014). However, in the absence of TTLL9, the abundance and flagellar localization of FAP234 is unaffected, although it no longer associates with the axonemal MTs. This suggest that FAP234 is not a MAP and that it requires TTLL9 for binding to MTs. Loss-of-function mutations in FAP234 or TTLL9, strongly decrease the level of glutamylation and appear to stabilize axonemal MTs (Kubo et al., 2014). Since FAP234 does not bind to MTs, this implies that the effect on the MT dynamics is mediated by TTLL9 and most likely tubulin glutamylation. In such a case, MT stabilization could be the result of reduced activity of severing enzymes, which are regulated by tubulin glutamylation and play an important role in controlling flagellar length (Casanova et al., 2009; Lacroix et al., 2010; Sharma et al., 2007). Thus, the main function of FAP234 appears to be the regulation of TTLL9 stability. In contrast, apart from stabilizing TTLL5, CSAP also regulates its activity. Moreover, the activating effect of CSAP seems specific to MTs and does not extend to other substrates, whether endogenous or ectopically expressed (Figures S5A–S5D).

The positive effect of CSAP on TTLL5 activity may result from its ability to load the enzyme onto the MTs as is the case for certain plus end-tracking proteins (+TIPs). For example, CLIP170 is not able to track the growing MT ends on its own but is loaded onto them by EB1 (Bieling et al., 2007). Therefore, CSAP might play a similar role in facilitating the interaction between TTLL5 and MTs. In support of this idea, when TTLL5 is expressed alone, it shows mostly diffused cytoplasmic staining, but in the presence of CSAP it re-localizes to MTs (Figure 5A). This increases the amount of the enzyme, which is in direct contact with the MTs, suggesting that CSAP-dependent activation is likely to stem from its ability to facilitate the interaction between the enzyme and the substrate. Importantly, in contrast to TTLL5 alone, which modifies both soluble tubulin and MTs, the complex modifies exclusively MTs (Figure 5B). Since all of the known effectors of glutamylation interact with MTs and not tubulin (Janke, 2014; Yu et al., 2015), this observation further underscores the importance of CSAP directing the activity toward MTs where functional consequences are expected.

CSAP directly stimulates TTLL5 glutamylase activity and promotes its association with MTs ultimately leading to increased severing (Figure 7), further substantiating the previously established link between glutamylation and severing (Lacroix et al., 2010; Sharma et al., 2007; Valenstein and Roll-Mecak, 2016). Our *in vitro* data suggest that CSAP needs to be expressed in

excess over TTLL5 for efficient activation. Interestingly, this is the case in most tissues where both proteins are expressed (Table S2) being particularly evident in brain, where CSAP has already been suggested to have physiologically relevant function (Backer et al., 2012). In view of our previously published observation that hyperglutamylation in brain leads to neurodegeneration (Rogowski et al., 2010) and our current findings that CSAP promotes glutamylation-dependent severing (Figure 7), it is tempting to propose that neurodegeneration might be caused by excessive severing activity. Thus, the regulation of glutamylation levels have to be tightly controlled, particularly in neurons, placing CSAP as a potentially important regulator of neuronal survival.

Several potential TTLL regulators have already been proposed, although their function remains to be confirmed. Indeed, one of the autonomously active glutamylases, TTLL6, apart from interacting with CSAP (Figure 6A), also binds to CEP41, a protein whose mutation causes Joubert syndrome (Lee et al., 2012). CEP41 appears to be critical for ciliary localization of TTLL6, but whether it also regulates the abundance and/or the enzymatic activity of TTLL6 remains yet unknown. Interestingly, CEP41 co-localizes with a mitotic spindle (Gache et al., 2010), but it is unclear whether this localization is the result of direct interaction with MTs. Future studies will establish whether CEP41, similarly to CSAP, directly interacts with MTs and acts as an activator of tubulin glutamylases.

In addition to increasing general tubulin glutamylases activity, CSAP also appears to stimulate elongase activity. This is particularly evident in the case of TTLL5 and TTLL7, which, when expressed alone, show a very weak elongation activity but become highly efficient in generating long glutamate chains in the presence of CSAP (Figure 6B). Nonetheless, the effect of CSAP does not extend to TTLL4, which is an "initiation only" enzyme and does not acquire the ability to elongate despite that its overall activity is increased. Thus, CSAP enhances activity but does not change intrinsic properties of the glutamylating enzymes.

Our work gives mechanistic insights into the regulation of tubulin glutamylation and identifies CSAP as a key activator of tubulin glutamylases. Recent studies described similar regulatory mechanism for two members of the vasohibin family, which are involved in the generation of another tubulin modification called detyrosination (Aillaud et al., 2017; Nieuwenhuis et al., 2017). This opens up the possibility that most, if not all, of the enzymes involved in the generation of tubulin code, are regulated in a similar manner. Overall, the mechanistic insights presented here will be of significance for understanding the pathophysiology of diseases caused by increased tubulin glutamylation such as male sterility, retinal degeneration, and neurodegeneration.

STAR★METHODS

Detailed methods are provided in the online version of this paper and include the following:

- KEY RESOURCES TABLE
- CONTACT FOR REAGENT AND RESOURCE SHARING
- EXPERIMENTAL MODEL AND SUBJECT DETAILS
- METHODS DETAILS
  - DNA constructs
  - RNA interference
  - RT-qPCR
  - Immunofluorescence, immunoprecipitation and pull-down
  - Cellular fractionation
  - Protein expression and purification
  - Live cell imaging and analysis of MT dynamics from EB3-GFP comets
  - Cell microscopy
  - Purification of tubulin and MT co-sedimentation assay
  - *In vitro* glutamylase assay
  - Tubulin co-polymerization assay
  - Protein expression in Sf9 cells
  - Immunoblot and severing quantifications
- QUANTIFICATION AND STATISTICAL ANALYSIS

SUPPLEMENTAL INFORMATION

Supplemental Information includes six figures and three tables and can be found with this article online at https://doi.org/10.1016/j.celrep.2018.10.095.

ACKNOWLEDGMENTS

This work was supported by CNRS, the University of Montpellier, the ATIP/Avenir, ANR Award 13-JSV2-0002, ARC Grant SFI20101201927, AFM, FRM, and Labex EpiGenMed. We thank N. Morin (CRBM, Montpellier, France), J.M. Andreu (CIB, Madrid, Spain), I. Cheeseman (MIT, Boston, MA, USA), L.M. Machesky (BI, Glasgow, UK), C.R. Thoma (ETH, Zurich, Switzerland), and K. Ikegami (IMIC, Hamamatsu, Japan) for providing reagents. We are grateful to V. Dulic (IGMM, Montpellier, France) and the staff at RIO Imaging facility of IGH for technical assistance, and we thank J. Gaertig (UGA, Athens, GA, USA) for critical reading of the manuscript. The monoclonal antibody 12G10 developed by J. Frankel and M. Nelson was obtained from the Developmental Studies Hybridoma Bank, developed under the auspices of the NICHD, and maintained by the University of Iowa.

AUTHOR CONTRIBUTIONS

Conceptualization, G.B. and K.R.; Methodology, G.B. and K.R.; Investigation, G.B., J.v.D., J.C., Y.L., G.M., A.L., S.v.d.L., and K.R.; Writing - Original Draft, G.B. and K.R.; Writing - Reviewing and Editing, G.B., S.v.d.L., and K.R.; Visualization, G.B. and S.v.d.L.; Supervision, G.B. and K.R.; Funding Acquisition, K.R.

DECLARATION OF INTERESTS

The authors declare no competing interests.

Received: October 16, 2017
Revised: December 22, 2017
Accepted: October 25, 2018
Published: December 4, 2018

REFERENCES

Aillaud, C., Bosc, C., Peris, L., Bosson, A., Heemeryck, P., Van Dijk, J., Le Friec, J., Boulan, B., Vossier, F., Sanman, L.E., et al. (2017). Vasohibins/SVBP are tubulin carboxypeptidases (TCPs) that regulate neuron differentiation. Science *358*, 1448–1453.

Applegate, K.T., Besson, S., Matov, A., Bagonis, M.H., Jaqaman, K., and Danuser, G. (2011). plusTipTracker: quantitative image analysis software for the measurement of microtubule dynamics. J. Struct. Biol. *176*, 168–184.

Ayala, R., Shu, T., and Tsai, L.H. (2007). Trekking across the brain: the journey of neuronal migration. Cell *128*, 29–43.

Backer, C.B., Gutzman, J.H., Pearson, C.G., and Cheeseman, I.M. (2012). CSAP localizes to polyglutamylated microtubules and promotes proper cilia function and zebrafish development. Mol. Biol. Cell *23*, 2122–2130.

Bedoni, N., Haer-Wigman, L., Vaclavik, V., Tran, V.H., Farinelli, P., Balzano, S., Royer-Bertrand, B., El-Asrag, M.E., Bonny, O., Ikonomidis, C., et al. (2016). Mutations in the polyglutamylase gene TTLL5, expressed in photoreceptor cells and spermatozoa, are associated with cone-rod degeneration and reduced male fertility. Hum. Mol. Genet. *25*, 4546–4555.

Bieling, P., Laan, L., Schek, H., Munteanu, E.L., Sandblad, L., Dogterom, M., Brunner, D., and Surrey, T. (2007). Reconstitution of a microtubule plus-end tracking system in vitro. Nature *450*, 1100–1105.

Bompard, G., Sharp, S.J., Freiss, G., and Machesky, L.M. (2005). Involvement of Rac in actin cytoskeleton rearrangements induced by MIM-B. J. Cell Sci. *118*, 5393–5403.

Bompard, G., Rabeharivelo, G., Cau, J., Abrieu, A., Delsert, C., and Morin, N. (2013). P21-activated kinase 4 (PAK4) is required for metaphase spindle positioning and anchoring. Oncogene *32*, 910–919.

Bonnet, C., Boucher, D., Lazereg, S., Pedrotti, B., Islam, K., Denoulet, P., and Larcher, J.C. (2001). Differential binding regulation of microtubule-associated proteins MAP1A, MAP1B, and MAP2 by tubulin polyglutamylation. J. Biol. Chem. *276*, 12839–12848.

Bowne-Anderson, H., Hibbel, A., and Howard, J. (2015). Regulation of microtubule growth and catastrophe: unifying theory and experiment. Trends Cell Biol. *25*, 769–779.

Casanova, M., Crobu, L., Blaineau, C., Bourgeois, N., Bastien, P., and Pagès, M. (2009). Microtubule-severing proteins are involved in flagellar length control and mitosis in trypanosomatids. Mol. Microbiol. *71*, 1353–1370.

Castoldi, M., and Popov, A.V. (2003). Purification of brain tubulin through two cycles of polymerization-depolymerization in a high-molarity buffer. Protein Expr. Purif. *32*, 83–88.

Gache, V., Waridel, P., Winter, C., Juhem, A., Schroeder, M., Shevchenko, A., and Popov, A.V. (2010). *Xenopus* meiotic microtubule-associated interactome. PLoS One *5*, e9248.

Gundersen, G.G., Khawaja, S., and Bulinski, J.C. (1989). Generation of a stable, posttranslationally modified microtubule array is an early event in myogenic differentiation. J. Cell Biol. *109*, 2275–2288.

Gupta, K.K., Paulson, B.A., Folker, E.S., Charlebois, B., Hunt, A.J., and Goodson, H.V. (2009). Minimal plus-end tracking unit of the cytoplasmic linker protein CLIP-170. J. Biol. Chem. *284*, 6735–6742.

Ikegami, K., Heier, R.L., Taruishi, M., Takagi, H., Mukai, M., Shimma, S., Taira, S., Hatanaka, K., Morone, N., Yao, I., et al. (2007). Loss of alpha-tubulin polyglutamylation in ROSA22 mice is associated with abnormal targeting of KIF1A and modulated synaptic function. Proc. Natl. Acad. Sci. USA *104*, 3213–3218.

Janke, C. (2014). The tubulin code: molecular components, readout mechanisms, and functions. J. Cell Biol. *206*, 461–472.

Janke, C., Rogowski, K., Wloga, D., Regnard, C., Kajava, A.V., Strub, J.M., Temurak, N., van Dijk, J., Boucher, D., van Dorsselaer, A., et al. (2005). Tubulin polyglutamylase enzymes are members of the TTL domain protein family. Science *308*, 1758–1762.

Kubo, T., Yanagisawa, H.A., Yagi, T., Hirono, M., and Kamiya, R. (2010). Tubulin polyglutamylation regulates axonemal motility by modulating activities of inner-arm dyneins. Curr. Biol. *20*, 441–445.

Kubo, T., Yanagisawa, H.A., Liu, Z., Shibuya, R., Hirono, M., and Kamiya, R. (2014). A conserved flagella-associated protein in *Chlamydomonas*, FAP234, is essential for axonemal localization of tubulin polyglutamylase TTLL9. Mol. Biol. Cell *25*, 107–117.

Lacroix, B., van Dijk, J., Gold, N.D., Guizetti, J., Aldrian-Herrada, G., Rogowski, K., Gerlich, D.W., and Janke, C. (2010). Tubulin polyglutamylation stimulates spastin-mediated microtubule severing. J. Cell Biol. *189*, 945–954.

Lee, J.E., Silhavy, J.L., Zaki, M.S., Schroth, J., Bielas, S.L., Marsh, S.E., Olvera, J., Brancati, F., Iannicelli, M., Ikegami, K., et al. (2012). CEP41 is mutated in Joubert syndrome and is required for tubulin glutamylation at the cilium. Nat. Genet. *44*, 193–199.

Lee, G.S., He, Y., Dougherty, E.J., Jimenez-Movilla, M., Avella, M., Grullon, S., Sharlin, D.S., Guo, C., Blackford, J.A., Jr., Awasthi, S., et al. (2013). Disruption of Ttll5/stamp gene (tubulin tyrosine ligase-like protein 5/SRC-1 and TIF2-associated modulatory protein gene) in male mice causes sperm malformation and infertility. J. Biol. Chem. *288*, 15167–15180.

Nieuwenhuis, J., Adamopoulos, A., Bleijerveld, O.B., Mazouzi, A., Stickel, E., Celie, P., Altelaar, M., Knipscheer, P., Perrakis, A., Blomen, V.A., and Brummelkamp, T.R. (2017). Vasohibins encode tubulin detyrosinating activity. Science *358*, 1453–1456.

O'Hagan, R., Piasecki, B.P., Silva, M., Phirke, P., Nguyen, K.C., Hall, D.H., Swoboda, P., and Barr, M.M. (2011). The tubulin deglutamylase CCPP-1 regulates the function and stability of sensory cilia in *C. elegans*. Curr. Biol. *21*, 1685–1694.

Ohta, S., Hamada, M., Sato, N., and Toramoto, I. (2015). Polyglutamylated tubulin binding protein C1orf96/CSAP is involved in microtubule stabilization in mitotic spindles. PLoS One *10*, e0142798.

Regnard, C., Fesquet, D., Janke, C., Boucher, D., Desbruyéres, E., Koulakoff, A., Insina, C., Travo, P., and Eddé, B. (2003). Characterisation of PGs1, a subunit of a protein complex co-purifying with tubulin polyglutamylase. J. Cell Sci. *116*, 4181–4190.

Rogowski, K., van Dijk, J., Magiera, M.M., Bosc, C., Deloulme, J.C., Bosson, A., Peris, L., Gold, N.D., Lacroix, B., Bosch Grau, M., et al. (2010). A family of protein-deglutamylating enzymes associated with neurodegeneration. Cell *143*, 564–578.

Sabo, Y., Walsh, D., Barry, D.S., Tinaztepe, S., de Los Santos, K., Goff, S.P., Gundersen, G.G., and Naghavi, M.H. (2013). HIV-1 induces the formation of stable microtubules to enhance early infection. Cell Host Microbe *14*, 535–546.

Sergouniotis, P.I., Chakarova, C., Murphy, C., Becker, M., Lenassi, E., Arno, G., Lek, M., MacArthur, D.G., Bhattacharya, S.S., Moore, A.T., et al.; UCL-Exomes Consortium (2014). Biallelic variants in TTLL5, encoding a tubulin glutamylase, cause retinal dystrophy. Am. J. Hum. Genet. *94*, 760–769.

Sharma, N., Bryant, J., Wloga, D., Donaldson, R., Davis, R.C., Jerka-Dziadosz, M., and Gaertig, J. (2007). Katanin regulates dynamics of microtubules and biogenesis of motile cilia. J. Cell Biol. *178*, 1065–1079.

Sirajuddin, M., Rice, L.M., and Vale, R.D. (2014). Regulation of microtubule motors by tubulin isotypes and post-translational modifications. Nat. Cell Biol. *16*, 335–344.

Steffen, A., Faix, J., Resch, G.P., Linkner, J., Wehland, J., Small, J.V., Rottner, K., and Stradal, T.E. (2006). Filopodia formation in the absence of functional WAVE- and Arp2/3-complexes. Mol. Biol. Cell *17*, 2581–2591.

Suryavanshi, S., Eddé, B., Fox, L.A., Guerrero, S., Hard, R., Hennessey, T., Kabi, A., Malison, D., Pennock, D., Sale, W.S., et al. (2010). Tubulin glutamylation regulates ciliary motility by altering inner dynein arm activity. Curr. Biol. *20*, 435–440.

Szyk, A., Deaconescu, A.M., Spector, J., Goodman, B., Valenstein, M.L., Ziolkowska, N.E., Kormendi, V., Grigorieff, N., and Roll-Mecak, A. (2014). Molecular basis for age-dependent microtubule acetylation by tubulin acetyltransferase. Cell *157*, 1405–1415.

Thoma, C.R., Matov, A., Gutbrodt, K.L., Hoerner, C.R., Smole, Z., Krek, W., and Danuser, G. (2010). Quantitative image analysis identifies pVHL as a key regulator of microtubule dynamic instability. J. Cell Biol. *190*, 991–1003.

Tort, O., Tanco, S., Rocha, C., Bièche, I., Seixas, C., Bosc, C., Andrieux, A., Moutin, M.J., Avilés, F.X., Lorenzo, J., and Janke, C. (2014). The cytosolic

carboxypeptidases CCP2 and CCP3 catalyze posttranslational removal of acidic amino acids. Mol. Biol. Cell *25*, 3017–3027.

Valenstein, M.L., and Roll-Mecak, A. (2016). Graded control of microtubule severing by tubulin glutamylation. Cell *164*, 911–921.

van Dijk, J., Rogowski, K., Miro, J., Lacroix, B., Eddé, B., and Janke, C. (2007). A targeted multienzyme mechanism for selective microtubule polyglutamylation. Mol. Cell *26*, 437–448.

van Dijk, J., Miro, J., Strub, J.M., Lacroix, B., van Dorsselaer, A., Edde, B., and Janke, C. (2008). Polyglutamylation is a post-translational modification with a broad range of substrates. J. Biol. Chem. *283*, 3915–3922.

Widlund, P.O., Podolski, M., Reber, S., Alper, J., Storch, M., Hyman, A.A., Howard, J., and Drechsel, D.N. (2012). One-step purification of assembly-competent tubulin from diverse eukaryotic sources. Mol. Biol. Cell *23*, 4393–4401.

Wolff, A., Houdayer, M., Chillet, D., de Néchaud, B., and Denoulet, P. (1994). Structure of the polyglutamyl chain of tubulin: occurrence of alpha and gamma linkages between glutamyl units revealed by monoreactive polyclonal antibodies. Biol. Cell *81*, 11–16.

Yu, I., Garnham, C.P., and Roll-Mecak, A. (2015). Writing and reading the tubulin code. J. Biol. Chem. *290*, 17163–17172.

STAR★METHODS

KEY RESOURCES TABLE

REAGENT or RESOURCE	SOURCE	IDENTIFIER
Antibodies		
Mouse monoclonal anti-Vinculin	Sigma Aldrich	V9131
Mouse monoclonal anti-β-tubulin (E7)	DSHB	E7
Mouse monoclonal anti-Acetylated-K40 (6-11B-1)	Sigma Aldrich	T7451
Mouse monoclonal anti-β-Actin (Clone AC-74)	Sigma Aldrich	A5316
Mouse monoclonal anti-GT335	Rogowski et al., 2010	N/A
Mouse monoclonal anti-HA (12CA5)	Sigma Aldrich	ROAHA Roche
Mouse monoclonal anti-HA (16B12)	Biolegend	MMS-101R-500
Rabbit polyclonal anti-TTLL5	Novus Biologicals	NBP2-32091
Rabbit polyclonal anti-GFP	Torrey Pines	TP401
Rabbit polyclonal anti-CSAP (N-16)	Santa Cruz	sc-137340
Mouse monoclonal anti-α tubulin (12G10)	DSHB	12G10
Rabbit polyclonal anti-β-tubulin (C102)	Gift from J. M. Andreu (Centro de Investigaciones Biológicas, Madrid, Spain)	N/A
Rabbit polyclonal anti-GST	Gift from N. Morin (CRBM, Montpellier, France)	N/A
Rabbit polyclonal anti-PolyE	Rogowski et al., 2010	N/A
Rabbit polyclonal anti-TTLL7	Gift from K. Ikegami (Department of Cellular and Molecular Anatomy and International Mass Imaging Center, Hamamatsu, Japan)	N/A
Rabbit polyclonal anti-TTLL11	van Dijk et al., 2007	N/A
Bacterial and Virus Strains		
BL21 Rosetta 2 (DE3)pLysS competent cells	Novagen	71403
Bac_His-hTTLL5	This paper	N/A
Bac_His-hTTLL7	This paper	N/A
Bac_His-TTLL11	This paper	N/A
Bac_GST	This paper	N/A
Bac_GST-CSAP	This paper	N/A
Bac_His-GFP	This paper	N/A
Bac_His-GFP-CSAP	This paper	N/A
Chemicals, Peptides, and Recombinant Proteins		
Taxol	Sigma Aldrich	T7191
Doxycycline	Sigma Aldrich	D1822
EX-CELL 420 SFM	Sigma Aldrich	14420C
jetPEI	Polyplus-transfection	101-10N
INTERFERin	Polyplus-transfection	409-10
Viromer GREEN	Lipocalyx	VG-01LB-00
QuikChange Site-Directed Mutagenesis	Agilent Technologies	200518
PrimeScript RT Reagent Kit	Takara	RR037B
LightCycler 480 SYBR Green I Master	Roche	04707516001
Protease Inhibitor Cocktail	Sigma Aldrich	P8340
Protein A–Agarose Fast Flow	Sigma Aldrich	P3476
GFP-Trap Agarose	Chromotek	gta-20
HIS-Select Cobalt Affinity Gel	Sigma Aldrich	H8162
Glutathione Sepharose 4 Fast Flow	Sigma Aldrich	GE17-5132-01
GST	This paper	N/A

(*Continued on next page*)

Continued

REAGENT or RESOURCE	SOURCE	IDENTIFIER
GST_Nt-CSAP	This paper	N/A
GST_Ct-CSAP	This paper	N/A
GST_CSAP	This paper	N/A
GST_CSAP-Δ178-204	This paper	N/A
GST_Nt-TTLL5	This paper	N/A
HA-GST_hTTLL5	This paper	N/A
His_GFP	This paper	N/A
His_GFP-CSAP	This paper	N/A
Nt-CLIP170_His	This paper	N/A
His_hTTLL5	This paper	N/A
His_hTTLL7	This paper	N/A
His_mTTLL11	This paper	N/A
Experimental Models: Cell Lines		
HEK293T	ATCC	CRL-11286
RPE-1	ATCC	CRL-4000
RPE-1 EB3-GFP	CR Thoma	Thoma et al., 2010
HCT 116	ATCC	CCL-247
U2OS	ATCC	HTB-96
Sf9	ATCC	CRL-1711
Oligonucleotides		
siRNA Luc: 5′-CGUACGCGGAAUACUUCGA-3′	This paper	siRNA Luc
siRNA TTLL5: 5′-CAGCAACAGACGACAGAAA-3′	This paper	siRNA TTLL5
siRNA CSAP: 5′-CAGCAUUACGAGCCAAGAA-3′	This paper	siRNA CSAP
TTLL5 Forward primer: CCATCCAGCCACATCAACCT	This paper	hTTLL5-fwd
TTLL5 Reverse primer: AGGACTGATGATGGGTCGGA	This paper	hTTLL5-rev
TTLL7 Forward primer: TGTGCGAATGGGTACAGAGA	This paper	hTTLL7-fwd
TTLL7 Reverse primer: GACACTTTCGCTTCCTGGAG	This paper	hTTLL7-rev
Recombinant DNA		
pCDNA5-FRT/TO_GFP-CSAP	This paper	N/A
pGEX-4T1_GST-Nt-CSAP	This paper	N/A
pGEX-4T1_GST-Ct-CSAP	This paper	N/A
pRK5_HA-GST	This paper	N/A
pRK5_HA-CSAP	This paper	N/A
pRK5_HA-Nt-CSAP	This paper	N/A
pRK5_HA-Ct-CSAP	This paper	N/A
pEGFP-N3_TTLL5	This paper	N/A
pGEX-4T1_GST-CSAP	This paper	N/A
pEGFP-C1_Nt-TTLL5	This paper	N/A
pEGFP-C1_Ct-TTLL5	This paper	N/A
pEGFP-C1_Nt-CSAP	This paper	N/A
pEGFP-C1_Ct-CSAP	This paper	N/A
pGEX-4T3_Nt-TTLL5	This paper	N/A
pRSET-B_GFP	This paper	N/A
pRSET-B_GFP-CSAP	This paper	N/A
pET28a_Nt-CLIP170-GFP	This paper	N/A
pEGFP-C1_CSAP Δ178-204	This paper	N/A
pGEX-4T1 CSAP Δ178-204	This paper	N/A
pEGFP-N3_hTTLL4	This paper	N/A

(*Continued on next page*)

Continued

REAGENT or RESOURCE	SOURCE	IDENTIFIER
pEGFP-N3_mTTLL6	van Dijk et al., 2007	N/A
pEGFP-N3_hTTLL7	This paper	N/A
pEGFP-N3_mTTLL11	van Dijk et al., 2007	N/A
pEGFP-N3_mTTLL13	van Dijk et al., 2007	N/A
pEGFP-N3_hTTL	This paper	N/A
pEGFP-N3_NAP2	This paper	N/A
pEGFP-N3_SET	van Dijk et al., 2008	N/A
pEGFP-N3_RanGAP1	van Dijk et al., 2008	N/A
pcDNA3.1_GFP-MAPD2	This paper	N/A
pcDNA3.1_GFP-Tau	This paper	N/A
pRK5_HA-GST-hTTLL5	This paper	N/A
pCDNA5-FRT/TO_mTTLL5-IRES-GFP	This paper	N/A
pACEBAC1_GST	This paper	N/A
pACEBAC1_GST-CSAP	This paper	N/A
pFastBAC HT_hTTLL5	This paper	N/A
pFastBAC HT_hTTLL7	This paper	N/A
pFastBAC HT_mTTLL11	This paper	N/A
pFastBAC HT_GFP	This paper	N/A
pFastBAC HT_GFP-CSAP	This paper	N/A
Software and Algorithms		
plusTipTracker	Applegate et al., 2011	Version 1.1.4
ImageJ	Open source	2.0.0-rc-68/1.52e

CONTACT FOR REAGENT AND RESOURCE SHARING

Further information and requests for resources and reagents should be directed to and will be fulfilled by the Lead Contact, Krzysztof ROGOWSKI (krzysztof.rogowski@igh.cnrs.fr).

EXPERIMENTAL MODEL AND SUBJECT DETAILS

Human retinal pigment epithelial (hTERT-RPE-1; RPE-1), human neuroblastoma (SH-SY5Y) and human colon cancer (HCT 116) cells were cultured in Dulbecco's Modified Eagle Medium: Nutrient Mixture F-12 (DMEM/F-12) supplemented with 10% fetal bovine serum (FBS) and antibiotics. RPE-1 stably expressing EB3-GFP (gift from C. R. Thoma, Institute of Molecular Health Sciences, ETH Zurich, Zurich, Switzerland) were maintained in similar medium supplemented with 0.4 mg/ml G418. RPE-1 stably expressing mTTLL5 IRES GFP under the control of doxycycline were obtained after co-transfecting RPE-1 FRT/T-Rex cells (gift from J. Pines, ICR, London, UK) with pCDNA5 FRT/TO Neo mTTLL5 IRES GFP along with pOG44 and selection with 0.4 mg/ml G418 and 10 μg/ml blasticidin. Human embryonic kidney (HEK293T) and human bone osteosarcoma epithelial (U2OS) cells were maintained in Dulbecco's Modified Eagle's medium (DMEM) supplemented with 10% FBS and antibiotics.

METHODS DETAILS

DNA constructs

Vectors encoding hTTLL4 (NM_014640), hTTLL5 (NM_015072) and hTTLL7 (NM_024686) fused to GFP were generated by PCR-based cloning into pEGFP-N3. A similar approach was used to clone GFP CSAP in pCDNA5 FRT/TO (Invitrogen) using pBABE-GFP CSAP, a generous gift from I. Cheeseman (MIT, Boston, USA), as template. Nt-TTLL5 (amino-acids 1-606), Ct-TTLL5 (607-1281) were cloned in pEGFP-C1. Corresponding Nt-TTLL5 cDNA was cloned in pGEX-4T3 (GE Healthcare). cDNAs corresponding to full-length, Nt- (1-133), Ct-CSAP (134-270) or CSAP Δ178-204, were introduced in pRK5-HA vector (gift from L. M. Machesky, Beatson Institute, Glasgow, UK), pEFGP-C1 and pGEX-4T1 vector (GE Healthcare) for respectively HA, GFP or GST tagged expression. hTTLL5 was also cloned in pRK5-HA GST vector. pRSET B vector (Invitrogen) encoding His GFP or His GFP tagged CSAP were generated by PCR-based cloning. GFP tagged mouse Nt-CLIP170 (1-350) was PCR cloned in pET28a vector. Site directed mutagenesis to generate inactive TTLL5 (E366G) was performed using QuickChange Site-Directed

Mutagenesis Kit (Agilent Technologies). Similar approach was used to generate internal deletions in CSAP cDNA sequence. mTTLL5 IRES GFP was PCR cloned into pCDNA5 FRT/TO Neo (gift from J. Pines, ICR, London, UK). For baculovirus generation, GST and GST CSAP were PCR cloned in pACEBAC1. GFP, GFP CSAP, hTTLL5, hTTLL7 and mTTLL11 were cloned by a similar approach in pFastBAC HT. Baculoviruses were generated using the Bac-to-Bac® Baculovirus Expression System (Invitrogen) following manufacturer's instructions. All constructs were sequenced. Remaining constructs were previously described (Bompard et al., 2013; van Dijk et al., 2008).

RNA interference

RPE-1 cells were transfected with 5 nM siRNA using INTERFERin (Polyplus-transfection, Ozyme) while SH-SY5Y cells were transfected with 20 nM siRNA using Viromer® GREEN (Lipocalyx) following manufacturer's instructions. Proteins were targeted with the following sequences:

Luciferase: 5′-CGUACGCGGAAUACUUCGA-3′
hTTLL5: 5′-CAGCAACAGACGACAGAAA-3′
CSAP: 5′-CAGCAUUACGAGCCAAGAA-3′

Cells were recovered 72 hours after siRNA transfection and analyzed by immunoblot or immunofluorescence.

RT-qPCR

Total RNA was isolated from all the different cell-lines with TRIzol reagent (Invitrogen). Reverse transcription was carried out with PrimeScript RT reagent kit (Takara) according to manufacturer's guidelines. Briefly, 500 ng of total RNA was reverse transcribed in presence of both random hexanucleotides and oligo(dT). Quantitative PCRs were performed using Lightcycler® 480 SYBR Green I Master mix (Roche) on Lightcycler apparatus (Roche). All primers used (STAR Methods and Table S3) are intronspanning to avoid amplification of genomic DNA. The relative amount of target cDNA was obtained by normalization using geometric averaging of multiple internal control genes (ACTB, HPRT, HMBS, GAPDH, and B2M).

Immunofluorescence, immunoprecipitation and pull-down

Immunofluorescence experiments were performed as described (Bompard et al., 2013).

All cell lines were DNA transfected using jetPEI (Polyplus-transfection, Ozyme) according to manufacturer's instructions. 24 hours post-transfection cells were either fixed and treated for immunofluorescence (RPE-1 and U2OS) or lysed (HEK293T) in RIPA derived lysis buffer (10 mM NaH_2PO_4, 100 mM NaCl, 5 mM EDTA, 1% Triton X-100, 0.5% NP-40, 80 mM β-Glycerophosphate, 1 mM DTT, 50 mM NaF, 1 mM Na_3VO_4 and protease inhibitor cocktail). Cleared lysates were either directly used for immunoblot analyses or immunoprecipitated by incubation with 12CA5 antibody crosslinked on protein A agarose beads (Amersham Biosciences) using dimethyl pimelimidate (DMP, Sigma Aldrich) or GFP-Trap® agarose beads (Chromotek) for one hour at 4°C. Beads were extensively washed with lysis buffer before immunoblot analysis.

For pull-down experiments, cleared lysates (500 μg) from HEK293T overexpressing various GFP-tagged proteins were incubated with 5 μg of GST or GST full-length, Nt-, Ct-CSAP or Δ178-204 immobilized on beads for one hour at 4°C. As previously beads were extensively washed with lysis buffer before immunoblot analysis.

Cellular fractionation

Tubulin and MTs were separated by incubating cells in MEM buffer (80 mM MES, 1 mM EGTA, 2 mM MgCl2, pH 6.8) supplemented with 4 M Glycerol, 0.1% Triton X-100, 1 mM Na_3VO_4 and protease inhibitor cocktail for 8 min at room temperature. MTs were pelleted at 16,000 g for 10 min at room temperature and resuspended in loading buffer. Supernatant (free tubulins) and pellet (polymerized tubulins) fractions were analyzed by immunoblot.

Protein expression and purification

Bacterially expressed glutathione S-transferase (GST)-fused full-length, Nt-, Ct-CSAP or Nt-TTLL5 were affinity-purified using glutathione beads (GE Healthcare). His-tagged proteins were purified on HIS-Select® Cobalt Affinity Gel (Sigma-Aldrich) as previously described (Bompard et al., 2005). Eluted proteins were dialysed against 50 mM Tris-HCl pH8, 100 mM NaCl, 1 mM DTT and concentrated using Amicon® Ultra centrifugal filters (Millipore).

Live cell imaging and analysis of MT dynamics from EB3-GFP comets

Movies were acquired with a DeltaVision OMX (GE Healthcare Life Sciences) microscope at 37°C using a 60 × silicone oil objective. 21 z stacks were acquired every second (frame rate 1 Hz) with an exposure time of 5 ms for 1 min. The 1,260 images per time lapse were deconvolved using Huggens Pro software (SVI). MT dynamics were determined by the analysis of EB3-GFP tracks from movies of reconstituted 3D images using plusTipTracker software (Version 1.1.4). Parameter used for all analysis were: maximum gap length, 15 frames; minimum track length, 3 frames; search radius range, 2-8 pixels; maximum forward angle, 30°; maximum backward angle, 10°; maximum shrinkage factor, 3; fluctuation radius, 2 pixels; pixel size, 133 nm and frame rate, 1 s.

Cell microscopy

Fixed cells were viewed using a Zeiss Axioimager Z1 with 63 × PLAN APO 1.4 oil lens. Micrographs were collected using either an Axiocam MRm 4 camera (Zeiss) or ORCA-Flash4.0 LT (Hamamatsu) with a structured illumination model (apotome) both driven by Zen2 software (Zeiss). Leica DM6000, with 40 × HCX PL APO 1.25-0.75 oil CS, was also used and images acquired with CoolSnap HQ (Roper Scientific) cameras driven by Metamorph 7.1 software (Molecular Devices). LSM 780 confocal microscope (Zeiss) fitted with 63 × PL-APO 1.4 oil DIC lens was also used.

Purification of tubulin and MT co-sedimentation assay

Tubulin was either prepared from porcine brain as described (Castoldi and Popov, 2003) or from Sf9 cells expressing or not His-tagged TTLL5 using GST TOG1 column as previously described (Widlund et al., 2012).

MTs were prepared by incubating tubulin in PEM buffer (80 mM PIPES, 2 mM EGTA, 1mM $MgCl_2$, pH 6.9) supplemented with 10 mM GTP and 20 μM taxol for 20 min at 37°C. MTs were pelleted at 100,000 g for 30 min at 37°C and resuspended in PEM containing 20 μM taxol.

Recombinant proteins were incubated with MTs in PEM buffer containing 20 μM taxol, 1 mM DTT and 100 or 300 mM KCl for 10 min at 37°C followed by a centrifugation through a cushion of 10% sucrose in PEM containing 20 μM taxol at 100,000 g for 15 min at 37°C. Supernatants were retrieved and pellets washed once with PEM buffer containing 20 μM taxol before being resuspended in equal volume of loading buffer.

In vitro glutamylase assay

HA GST TTLL5 purified from transfected HEK293T cells was used for the determination of glutamylase activity as previously described (van Dijk et al., 2007). Briefly, reaction mixture (15 μl: 50 mM Tris [pH7], 2.4 mM $MgCl_2$, 0.5 mM DTT, 4 μM taxol, 0.4 mM ATP, 8.9 μM L-[^{3}H]-glutamate, 30 Ci/mmol; American Radiolabeled Chemicals, Inc) containing 1 μM taxol-stabilized MTs, 0.025 μM HA GST TTL5 and various amount of His GFP or His GFP CSAP, produced in insect cells, were incubated at 37°C for 3 hours. Quantifications were done by scintillation counting of the tubulin bands after SDS-PAGE and electrotransfer onto nitrocellulose.

Tubulin co-polymerization assay

Tubulin bellow critical concentration (7.5 μM) was incubated with 1 μM of recombinant proteins for 30 min at 30°C in PEM buffer supplemented with 1 mM GTP and 1 mM DTT. MTs were precipitated by 100,000 g centrifugation at 30°C for 15 min through a cushion of 10% sucrose in PEM containing 1 mM GTP. Supernatant containing free tubulins and pellet, washed once with PEM supplemented with 20 μM taxol, containing MTs were retrieved and analyzed by immunoblots.

Protein expression in Sf9 cells

His GFP, His GFP CSAP, GST, GST CSAP and His TTLL5 were expressed in Sf9 cells after infection with baculoviruses. Consequences of single or combined expression on endogenous tubulin glutamylation were analyzed by immunoblot from total cell lysates three days after infection.

Immunoblot and severing quantifications

Immunoblot quantification was performed on underexposed film scans using ImageJ (2.0.0-rc-68/1.52e) software. Quantification of MT severing was performed by blindly counting transfected cells presenting visually significant drop (around 50%) of tubulin intensity by at least two independent persons.

QUANTIFICATION AND STATISTICAL ANALYSIS

Statistical differences were assessed with an unpaired Student's t test (two tailed). Calculations were performed using Prism 7, version 7.0c (GraphPad). Data are represented as means ± standard errors of the mean (SEM) or standard deviations (SD) otherwise mentioned. n indicated the number of individual experiments. *P value*s are indicated within figure legends and on figures as followed: * < 0.05, ** < 0.01, *** < 0.001. Numbers of counted cells are indicated within figure legends when required.